

1410

## A new nose extension method for whistlers

L. C. BERNARD

Radioscience Laboratory, Stanford University, Stanford,  
California 94305, U.S.A.

(Received 14 August 1972; in revised form 16 October 1972)

**Abstract**—The dispersion  $D = tf^{1/2}$  of ducted whistlers is approximated by  $D = D_0(f_{HE} - Af)/(f_{HE} - f)$ , where  $f$  is the whistler frequency,  $t$  the travel time and  $f_{HE}$  the minimum electron gyrofrequency along the propagation path.  $D_0$  is the zero-frequency or Eckersley dispersion, and the parameter  $A$  depends on detailed distribution of electron gyrofrequency and plasma frequency along the path. Based on this approximate dispersion function, methods are developed by which the nose frequency  $f_n$  and the travel time at the nose  $t_n$  can be calculated from measurements of travel time at any two frequencies. The formulas for  $f_n$  and  $t_n$  involve only simple algebraic functions and therefore permit speedy data processing with high precision. When applied to nose whistlers, this method often allows better estimates of  $f_n$  than are possible by direct measurements. This is particularly important in measurements of magnetospheric east-west convection electric fields using cross- $L$  drifts of whistler ducts.

### 1. INTRODUCTION

SINCE the early 1950's, the ground-based whistler technique has provided a unique and powerful tool for studies of the structure and dynamics of the inner magnetosphere. Recently there have been detailed whistler studies of the plasma distribution in the magnetosphere (ANGERAMI and CARPENTER, 1966; CARPENTER, 1966; PARK and CARPENTER, 1970), of cross- $L$  drift motions (CARPENTER *et al.*, 1972) and of ionosphere-magnetosphere interactions (PARK, 1970, 1972b). An important practical limitation in some of these studies is the fact that many observed whistler curves are only partially defined on frequency time records. In particular, the observational curves frequently do not exhibit a 'nose frequency' or frequency of minimum group delay. Since the nose frequency  $f_n$  and the associated travel time at the nose  $t_n$  are of fundamental interest in magnetospheric diagnostics using whistlers, it is necessary to develop curve fitting methods that will permit the recovery of equivalent information from partially defined whistler curves.

SMITH and CARPENTER (1961), BRICE (1965) and DOWDEN and ALLCOCK (1971) have developed methods of extrapolating the nose frequency and the travel time at the nose from non-nose whistlers. Calculations of whistler path latitude and electron concentration along the path can then proceed as in the case of nose whistlers (e.g. PARK, 1972a). The Smith and Carpenter method involves somewhat laborious processes of evaluating elliptical integrals which are used to approximate whistler dispersion  $D \equiv t\sqrt{f}$ . In the Dowden and Allcock method, the function  $Q \equiv 1/D$  is approximated by a linear function of frequency. This method has the advantage of mathematical simplicity, but requires a large number of scaled data points. The graphical method of Brice is simple to use, but is not well suited for processing large quantities of data when high precision is required. In this paper we develop methods of extrapolating  $f_n$  and  $t_n$  from two points on the whistler trace and involving only simple algebraic functions. The main advantage of these methods is that they allow speedy data processing with high precision.

The first problem in extrapolating whistler traces is to find a suitable mathematical expression for dispersion  $D = t\sqrt{f}$ . The whistler travel time is given by (see, for example, HELLIWELL, 1965)

$$t = \frac{1}{c} \int \mu_g ds = \frac{1}{2c} \int \frac{f_p f_H}{f^{1/2}(f_H - f)^{3/2}} ds \quad (1)$$

where  $c$  = speed of light in free space,  $\mu_g$  = group refractive index,  $f$  = wave frequency,  $f_p$  = plasma frequency,  $f_H$  = electron gyrofrequency,  $ds$  = an element of path length along a geomagnetic field line. The integral is over the entire field-line path. Using equation (1),  $D$  can be written

$$D = \frac{1}{2c} \int \frac{f_p f_H}{(f_H - f)^{3/2}} ds. \quad (2)$$

Unfortunately, this integral equation has no analytical solution for reasonable models of  $f_p$ , and a suitable function must be found to approximate it.

The plan of the paper is as follows. Equation (2) is divided into a 'magnetospheric' path above 1000 km altitude and two conjugate 'ionospheric' paths below 1000 km. First, ignoring the ionosphere, an approximate formula for  $D$  is found in Section 2. This formula is then used to develop the nose extension methods in Section 3. Corrections for dispersion in the ionosphere are then considered in Section 4. Section 5 discusses applications of the nose extension methods and expected errors.

## 2. APPROXIMATE FORMULA FOR WHISTLER DISPERSION

We substitute normalized frequencies  $\Lambda = f/f_{HE}$ ,  $b = f_H/f_{HE}$  and  $\varphi = f_p/f_{pE}$  into equation (2) to obtain

$$D = \frac{f_{pE}}{2cf_{HE}^{1/2}} \int \frac{\varphi b}{(b - \Lambda)^{3/2}} ds \quad (3)$$

where the subscript  $E$  refers to the top of the field-line path. Since  $\Lambda < b$ , we make a Taylor expansion:

$$b(b - \Lambda)^{-3/2} = b^{-1/2} \left( 1 + \frac{3}{2} \frac{\Lambda}{b} + \frac{15}{8} \frac{\Lambda^2}{b^2} + \dots \right).$$

The integral in equation (3) is then written as

$$I = d_0 + d_1 \Lambda + d_2 \Lambda^2 + \dots + d_k \Lambda^k + \dots$$

where

$$d_0 = \int \frac{\varphi}{b^{1/2}} ds, \quad d_1 = \frac{3}{2} \int \frac{\varphi}{b^{3/2}} ds, \quad d_2 = \frac{15}{8} \int \frac{\varphi}{b^{5/2}} ds, \dots$$

The relative values of the coefficients  $d_k$  can be estimated by inspection. As  $b(s) \geq 1$  along the whistler path, the integrals in the expressions of the coefficients  $d_k$  decrease with increasing  $k$ , but not very fast because the major contribution of the dispersion comes from the region around the Equator, that is where  $b$  is close to unity. Moreover the multiplication factors of these integrals increase with increasing  $k$ . Therefore we do not expect that the expansion of  $I$  as written converges very fast

and we try an empirical approximation by truncating the expansion at some term and replacing all the remaining  $d_n$  by an average value  $d$ :

$$I \cong d_o + d\Lambda(1 + \Lambda + \Lambda^2 + \dots) = d_o + d\left(\frac{\Lambda}{1 - \Lambda}\right).$$

The justification for this approximation is that it leads to an approximate dispersion function with satisfactory accuracy (see Fig. 2).

With this approximation for the integral in equation (3), we can write

$$\begin{aligned} D &= D_o \frac{f_{HE} - Af}{f_{HE} - f} & (4) \\ D_o &= \frac{f_{PE} d_o}{2cf_{HE}^{1/2}} \\ A &= \frac{d_o - d}{d_o}. \end{aligned}$$

In the  $(f, D)$  plane,  $D(f)$  as given by equation (4) is merely a hyperbola and we shall hereafter refer to it as the hyperbola approximation to the whistler dispersion.

$D_o$  is the zero-frequency or ECKERSLEY (1935) dispersion. The value of  $A$  depends on the magnetic shell coordinate of the whistler path and on the variation of  $f_H$  and  $f_p$  along the path.

To evaluate  $A$ , we first differentiate equation (1) with respect to  $f$  and write

$$\frac{dD}{df} = \frac{dt}{df} \sqrt{f} + \frac{D}{2f}.$$

At the nose frequency,  $dt/df = 0$ , and the above equation reduces to

$$\left(\frac{dD}{df}\right)_{f_n} = \frac{D_n}{2f_n}. \quad (5)$$

A substitution of equation (4) into equation (5) yields

$$A = \frac{3\Lambda_n - 1}{\Lambda_n(1 + \Lambda_n)} \quad (6)$$

where  $\Lambda_n = f_n/f_{HE}$ . Substituting equation (6) back into equation (4), we obtain a useful relationship at the nose frequency

$$\frac{D_n}{D_o} = \frac{2}{1 + \Lambda_n}. \quad (7)$$

Equations (4) and (7) can be combined to obtain another useful expression for normalized travel time as a function of normalized frequency

$$\frac{t}{t_n} = \frac{1}{2\sqrt{ff_n}} \frac{(1 + \Lambda_n) - (3\Lambda_n - 1)(ff_n)}{1 - \Lambda_n(ff_n)}. \quad (8)$$

PARK (1972a) has calculated  $\Lambda_n$  as a function of whistler path latitude for several different models of plasma distribution along the field line paths. His results for a

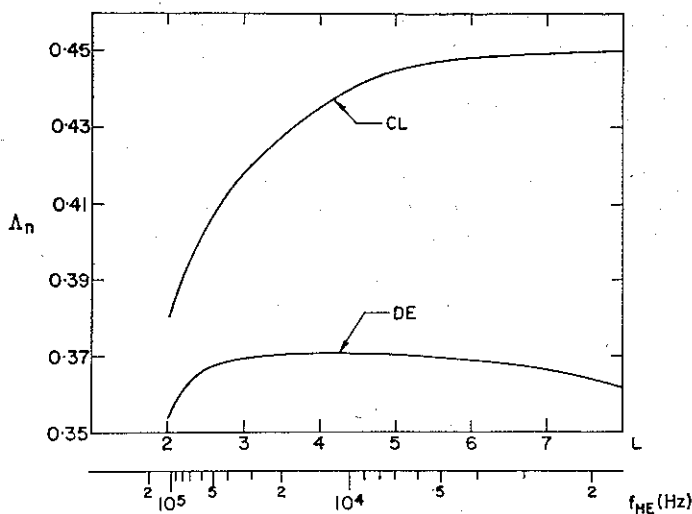


Fig. 1. A plot of normalized nose frequency  $\Lambda_n$  vs.  $L$  for a diffusive equilibrium model ( $T_e = T_i = 1600^\circ\text{K}$ ; 90%  $\text{O}^+$ , 8%  $\text{He}^+$  and 2%  $\text{He}^+$  at 1000 km), and a collisionless model ( $T_e = T_i = 3200^\circ\text{K}$ ; 100%  $\text{H}^+$  at 1000 km) of field-line plasma distribution. Equatorial electron gyrofrequency is shown at the bottom.

diffusive equilibrium model ( $T_e = T_i = 1600^\circ\text{K}$ ; 90%  $\text{O}^+$ , 8%  $\text{H}^+$  and 2%  $\text{He}^+$  at 1000 km altitude) and an idealized collisionless model ( $T_e = T_i = 3200^\circ\text{K}$ ; 100%  $\text{H}^+$  at 1000 km altitude) are plotted in Fig. 1. He also showed that changes in temperature and ion composition have little effect on  $\Lambda_n$ .

Figure 2 illustrates the error due to the approximation by equation (4). The broken curve is a plot of  $D/D_0$  vs. normalized frequency  $\Lambda$  as given by equation (4) and is to be compared with the solid curve for exact values of  $D/D_0$  obtained by numerically integrating equation (2). The error is less than 1 per cent. The dashed curve shows the approximate dispersion by an elliptical integral suggested by SMITH and CARPENTER (1961). The fact that the present approximation is better can be attributed to the use of parameter  $A$  which takes the magnetospheric model into account in the first order. Similar comparisons have been made for different models of field-line plasma distribution including the collisionless model of ANGERAMI (1966), a constant density model and a gyro-frequency model. In each case, the error due to the approximation of equation (4) remains less than 1 per cent for  $\Lambda < 0.5$ .

### 3. NOSE EXTENSION METHOD

In this section, we develop a method of extrapolating  $f_n$  and  $t_n$  from measurements of  $f$  and  $t$  at two points on the whistler trace.

Let  $R$  be the ratio of dispersion at the upper and lower frequencies, i.e.

$$R = \frac{D_U}{D_L} = \frac{t_U \sqrt{f_U}}{t_L \sqrt{f_L}}$$

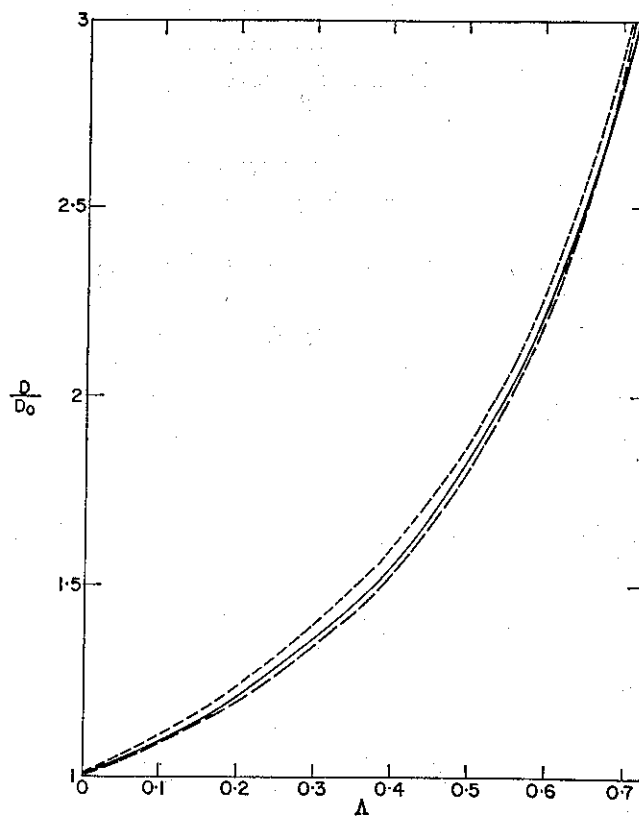


Fig. 2. A plot of normalized dispersion  $D/D_0$  vs. normalized whistler frequency  $\Lambda$ . The solid curve is calculated for a whistler propagating along an  $L = 3$  path assuming the diffusive equilibrium model of Fig. 1. The broken curve shows the hyperbola approximation used in this paper, and the dashed curve represents Smith and Carpenter's approximation by an elliptical integral.

From equation (4) we can write

$$R = \frac{\left(\frac{f_{HE} - Af_U}{f_{HE} - f_U}\right)}{\left(\frac{f_{HE} - Af_L}{f_{HE} - f_L}\right)}$$

and rearrange the terms to obtain

$$f_{HE}^2 - f_0 f_{HE} + Af_U f_L = 0 \tag{9}$$

where

$$f_0 = \frac{(R - A)f_U + (AR - 1)f_L}{R - 1}$$

Since  $\Lambda_n$ , and therefore  $A$ , varies only slowly with  $f_{HE}$  (see Fig. 1), we solve the

quadratic equation for  $f_{HE}$  assuming that  $A$  is constant with  $f_{HE}$ :

$$f_{HE} = \frac{f_o + \sqrt{f_o^2 - 4Af_{UL}}}{2}$$

Hence

$$f_n = \Lambda_n \frac{f_o + \sqrt{f_o^2 - 4Af_{UL}}}{2} \quad (10)$$

For ease of computation, the formula can be simplified by using the fact that  $Af_{UL} \ll f_{HE}^2$ . We then have

$$f_n \cong \Lambda_n \left( f_o - \frac{Af_{UL}}{f_o} \right) \quad (11)$$

To find  $t_n$ , we start with the relation

$$t_n = \frac{D_n}{\sqrt{f_n}} \quad (12)$$

$D_n$  can be expressed in terms of dispersion at any frequency by substituting equation (4) into equation (7).

$$D_n = D \frac{2}{(1 + \Lambda_n)} \frac{(f_{HE} - f)}{(f_{HE} - Af)}$$

Equation (12) then becomes

$$t_n = \frac{2}{\sqrt{f_n}} \frac{D}{(1 + \Lambda_n)} \frac{(f_n - \Lambda_n f)}{(f_n - A\Lambda_n f)} \quad (13)$$

For  $D$  and  $f$ , either upper or lower-frequency values may be used.

The values of  $\Lambda_n$  and  $A$  to be used in equations (10) and (13) can be obtained from Fig. 1 and equation (6). Figure 1 shows that  $\Lambda_n$  depends on the  $L$  value of the whistler path, which is not known *a priori*. However, the  $L$  dependence of  $\Lambda_n$  and therefore of  $A$  is weak enough so that in practice, it can be usually ignored without introducing serious errors. For example, for a diffusive equilibrium model,  $\Lambda_n = 0.369$  and  $A = 0.212$  give satisfactory results for a wide range of  $L$  values. In principle, errors due to ignoring the  $L$  dependence of  $\Lambda_n$  can be removed by an iteration process in which a new value of  $\Lambda_n$  is obtained from the values of  $f_n$  and  $L$  calculated in the previous step. (The  $L$  value can be calculated from  $f_n$  by methods described by PARK, 1972a.)

#### 4. EFFECTS OF THE IONOSPHERE

The conjugate ionospheres contribute a small additional dispersion to the whistlers propagating through them. This can be taken into account by an additive term  $D_i$  in equation (4).

$$D = D_i + D_o \frac{(f_{HE} - Af)}{(f_{HE} - f)} \quad (14)$$

The value of  $D_i$  may vary from 4 to 12  $\text{sec}^{1/2}$  depending on ionospheric conditions and can be estimated in the manner prescribed by PARK (1972a).

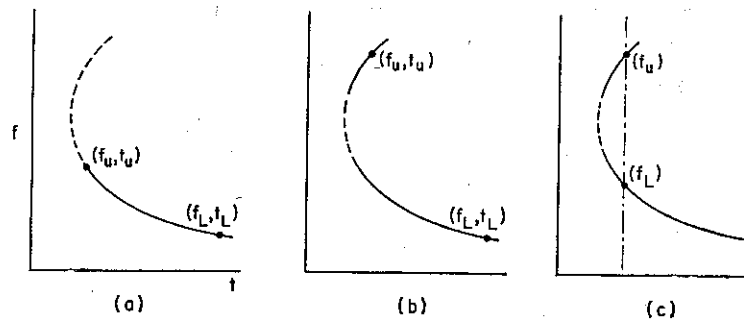


Fig. 3. A sketch of whistler spectrograms illustrating applications of nose extension methods developed in this paper. Portions of whistlers not visible or otherwise obscured are shown dashed.

In the nose extension method,  $D_i$  can be subtracted from measured values of  $D_U$  and  $D_L$  before the formulas in the previous section are applied. An alternative method is to use the measured values of  $D_U$  and  $D_L$ , but adjust the value of  $\Lambda_n$  to account for the ionospheric dispersion. Under 'average' ionospheric conditions,  $\Lambda_n = 0.377$  and  $\Lambda_n = 0.48$  give satisfactory results for a diffusive equilibrium model and a collisionless model of field-line plasma distribution, respectively.

##### 5. APPLICATIONS OF THE NOSE EXTENSION METHOD

When a whistler nose is not visible on a frequency-time spectrogram, equations (10) and (13) may be used to calculate  $f_n$  and  $t_n$  from any two pairs of measurements  $(f_U, t_U)$  and  $(f_L, t_L)$  on the visible portions of the trace. Figure 3 illustrates three different situations in which  $f_n$  and  $t_n$  cannot be measured directly. Portions of whistler traces not visible or otherwise obscured are shown dashed.

If  $f_U < f_n$ , as in the case of Fig. 3(a), uncertainties in the extrapolated  $f_n$  and  $t_n$  depend critically on the value of  $R$ . When  $R$  approaches 1, a small error in  $R$  results in large errors in  $f_n$  and  $t_n$  because of the denominator  $(R - 1)$  in the expression for  $f_o$ . For a study of errors in the extension method, equations (10) and (13) have been applied to four well-defined nose whistlers with  $f_n$  ranging from  $\sim 5$  to 20 kHz. The whistlers were scaled at several points along the traces below  $f_n$  and  $t_n$ . Figures 4 and 5 show scatter plots of  $\Delta f_n/f_n$  and  $\Delta t_n/t_n$  against  $R$ . The error decreases with increasing  $R$  and is better than  $\sim 3$  per cent for  $R > 1.1$ . The triangles connected by solid lines (whistler 5) were obtained by applying the same extension methods to a theoretically calculated whistler trace assuming a diffusive equilibrium distribution of plasma along field lines. In this case, the error is attributable to the approximations made in developing the extension method, and the unsmoothness of data points is due to roundoff errors.

It follows that when  $f_U < f_n$ , it is advantageous to maximize  $R$ . This can be accomplished by choosing  $f_U$  as high as possible and  $f_L$  as low as possible. However, this should be weighed against increased measurement errors when the trace is nearly vertical or horizontal. If  $f_U > f_n$  and  $f_L < f_n$ , as illustrated in Fig. 3(b), the magnitude of  $R$  is usually not an important consideration. Care should be taken, however, to ensure that the trace above  $f_n$  is a part of the whistler, and is not a whistler-triggered emission.

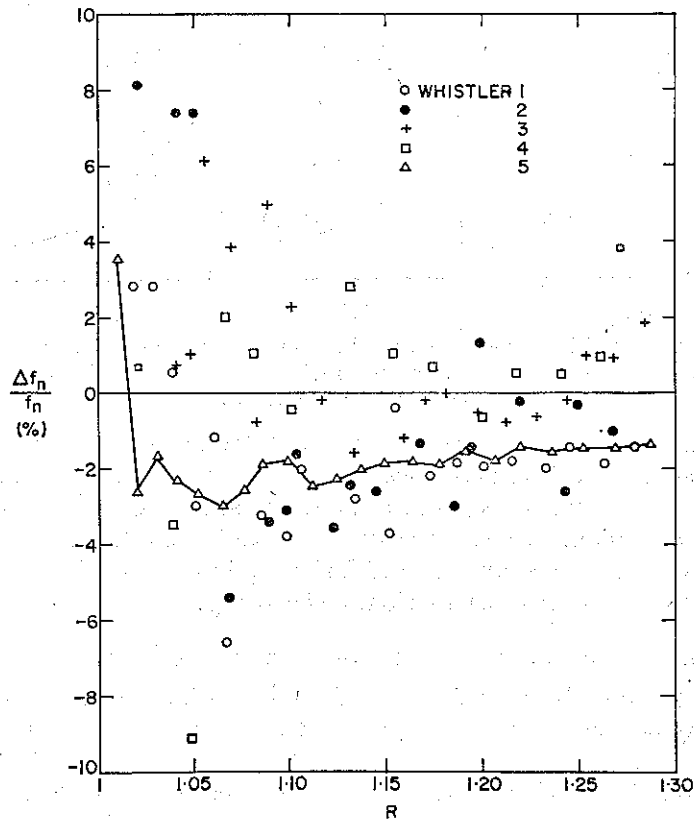


Fig. 4. Percentage error in extrapolated values of  $f_n$  plotted against  $R \equiv D_U/D_L$  for four actual nose whistlers (whistlers 1-4) and a theoretical whistler (whistler 5) based on the diffusive equilibrium model of Fig. 1. In all cases,  $f_U f_n < 1$  and  $f_U/f_n \sim \frac{1}{3}$ , the whistler parameters are as follows: whistlers 1:  $t_n = 1.81 \text{ s} \pm 1\%$ ,  $f_n = 5.48 \text{ kHz} \pm 3\%$ ; whistler 2:  $t_n = 0.74 \text{ s} \pm 1\%$ ,  $f_n = 10.82 \text{ kHz} \pm 3\%$ ; whistler 3:  $t_n = 0.676 \text{ s} \pm 1.5\%$ ,  $f_n = 13.08 \text{ kHz} \pm 3\%$ ; whistler 4:  $t_n = 0.444 \text{ s} \pm 1.5\%$ ,  $f_n = 19.60 \text{ kHz} \pm 3\%$ .

If one is interested in  $f_n$  only, the extension method can be simplified substantially by choosing two frequencies with the same travel time, as illustrated in Fig. 3(c). This eliminates the need for identifying causative spherics and measuring  $t_U$  and  $t_L$ . Equation (10) still applies in this case, but  $R$  becomes simply  $\sqrt{f_U/f_L}$ . Many nose whistlers have sufficient definition to allow direct measurements of  $t_n$  with satisfactory accuracy, but not  $f_n$ . In such cases, this interpolation method can be used to obtain a relatively accurate estimate of  $f_n$ .

Figure 6 shows a comparison between direct measurements of  $f_n$  (crosses) and the results of interpolation (dots). The measured whistlers were recorded at Eights, Antarctica on 12 April 1965, from 1336 to 1343 UT, and from standard techniques involving comparison of the frequency-time curves of successive events, were found to be propagating along the same magnetospheric duct. The standard deviations of data points is 75.9 Hz for direct measurements and 25.7 Hz for interpolated values. The mean value of the data points is  $\sim 4.60 \text{ kHz}$ . Therefore, we expect in 95 per cent



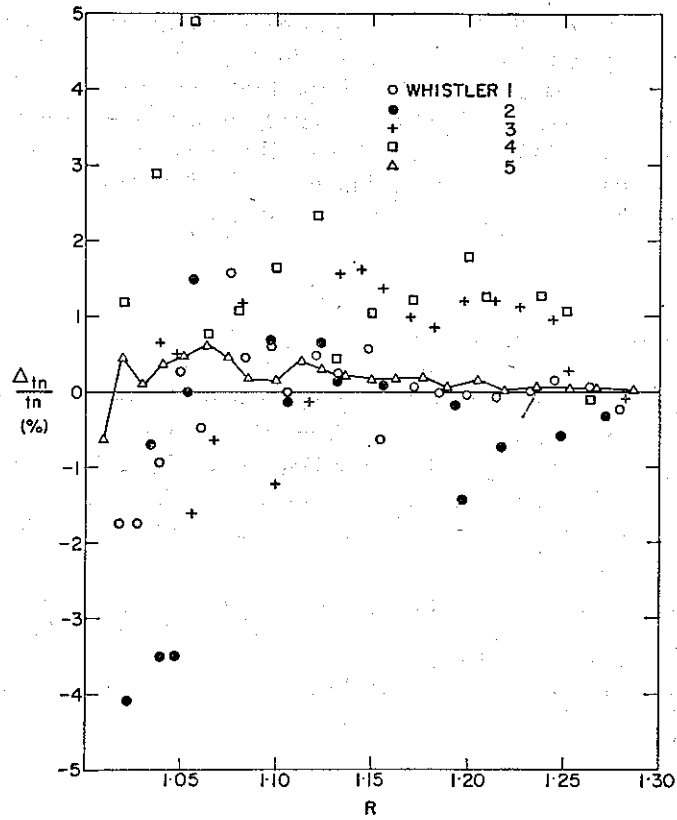


Fig. 5. A plot similar to Fig. 4 but for  $t_n$ .

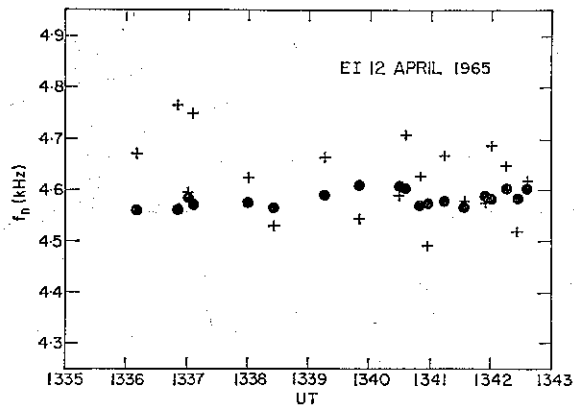


Fig. 6. A plot of  $f_n$  vs. UT for nose whistlers recorded at Eights, Antarctica on 12 April 1965. These whistlers were found to propagate along the same whistler duct, and the scatter of data points is attributed to measurement errors. The crosses represent values obtained by direct measurements and the dots by the extension method.

of the cases an error of  $2 \times 75.9/4600 \sim 3$  per cent, for direct measurements and  $2 \times 25.7/4600 \sim 1$  per cent, for interpolated values.

The interpolated scheme has played an important role in determining the east-west component of magnetospheric electric field from cross- $L$  motions of whistler ducts (CARPENTER *et al.*, 1972). The value of the westward convection electric field  $E_w$  is deduced from the variation in time of the  $L$  value of the duct location, or equivalently the variation in time of the nose frequency.

$$E_w = C \frac{d(f_n^{2/3})}{dt}$$

where  $C$  is a constant. The method has the particular advantage of not requiring knowledge of the times of origin of successive whistler events.

The precision in measurement of  $f_n$  is of fundamental importance in obtaining precise values of  $E_w$ , particularly because a derivative is involved. Use of the interpolation scheme permitted observation of variations in  $E_w$  which would not have been detectable otherwise. In some cases it has been possible to resolve fluctuations  $E_w$  with period  $T \sim 12$  min and r.m.s. amplitude as low as 0.03 mV/m (N. SEELY, private communication).

*Acknowledgements*—The author is grateful to Prof. R. A. HELLIWELL for helpful discussions, to Drs. C. G. PARK and D. L. CARPENTER for invaluable comments and careful reading of the manuscript, and to Mr. N. SEELY for making available to him data on east-west convection electric field measurements. This research was supported in part by the National Science Foundation under grants GA-28042 and GA-32590X, and in part by the Office of Polar Programs of the National Science Foundation under grant GV-28840X.

#### REFERENCES

- |  |       |   |
|--|-------|---|
| ANGERAMI J. J. and CARPENTER D. L.                       | 1966  | <i>J. geophys. Res.</i> <b>71</b> , 711.  |
| BRICE N.   | 1965  | <i>J. atmos. terr. Phys.</i> <b>27</b> , 1.                                     |
| CARPENTER D. L.  | 1966  | <i>J. geophys. Res.</i> <b>71</b> , 693.  |
| CARPENTER D. L., STONE K., SIREN J.<br>and CRYSTAL T. L. | 1972  | <i>J. geophys. Res.</i> <b>77</b> , 2819.                                       |
| DOWDEN R. L. and ALLCOCK G. MCK.                         | 1971  | <i>J. atmos. terr. Phys.</i> <b>33</b> , 1125.                                  |
| ECKERSLEY T. L.  | 1935  | <i>Nature, Lond.</i> <b>135</b> , 16.   |
| HELLIWELL R. A.  | 1965  | <i>Whistlers and Related Ionospheric Phenomena</i> . Stanford University Press. |
| PARK C. G.   | 1970  | <i>J. geophys. Res.</i> <b>75</b> , 4249.                                       |
| PARK C. G.   | 1972b | <i>J. geophys. Res.</i> (in press).   |
| PARK C. G. and CARPENTER D. L.                           | 1970  | <i>J. geophys. Res.</i> <b>75</b> , 3825.                                       |
| SMITH R. L. and CARPENTER D. L.                          | 1961  | <i>J. geophys. Res.</i> <b>66</b> , 2582.                                       |

*Reference is also made to the following unpublished material:*

- |                |       |  |
|----------------|-------|--|
| ANGERAMI J. J. | 1966  | Tech. Rept. 3412-7, Stanford University. |
| PARK C. G.     | 1972a | Tech. Rept. 3454-1, Stanford University. |